Methods xxx (2017) xxx–xxx

Contents lists available at ScienceDirect

Methods

journal homepage: www.elsevier.com/locate/ymeth

Effect of heparin and heparan sulphate on open promoter complex formation for a simple tandem gene model using *ex situ* atomic force microscopy

Oliver Chammas [a,b], William A. Bonass [a], Neil H. Thomson [a,b,*]

[a] Department of Oral Biology, School of Dentistry, St James's University Hospital, University of Leeds, Leeds LS9 7TF, UK
[b] School of Physics and Astronomy, Woodhouse Lane, University of Leeds, LS2 9JT, UK

ARTICLE INFO

Article history:
Received 25 January 2017
Received in revised form 10 April 2017
Accepted 14 April 2017
Available online xxxx

Keywords:
Heparin
Heparan sulphate
E. coli RNA polymerase
DNA
Mica
AFM

ABSTRACT

The influence of heparin and heparan sulphate (HepS) on the appearance and analysis of open promoter complex (RP_o) formation by *E. coli* RNA polymerase (RNAP) holoenzyme (σ^{70}RNAP) on linear DNA using *ex situ* imaging by atomic force microscopy (AFM) has been investigated. Introducing heparin or HepS into the reaction mix significantly reduces non-specific interactions of the σ^{70}RNAP and RNAP after RP_o formation allowing for better interpretation of complexes shown within AFM images, particularly on DNA templates containing more than one promoter. Previous expectation was that negatively charged polysaccharides, often used as competitive inhibitors of σRNAP binding and RP_o formation, would also inhibit binding of the DNA template to the mica support surface and thereby lower the imaging yield of active RNAP-DNA complexes. We found that the reverse of this was true, and that the yield of RP_o formation detected by AFM, for a simple tandem gene model containing two λ_{PR} promoters, increased. Moreover and unexpectedly, HepS was more efficient than heparin, with both of them having a dispersive effect on the sample, minimising unwanted RNAP-RNAP interactions as well as non-specific interactions between the RNAP and DNA template. The success of this method relied on the observation that *E. coli* RNAP has the highest affinity for the mica surface of all the molecular components. For our system, the affinity of the three constituent biopolymers to muscovite mica was RNAP > Heparin or HepS > DNA. While we observed that heparin and HepS can inhibit DNA binding to the mica, the presence of *E. coli* RNAP overcomes this effect allowing a greater yield of RP_os for AFM analysis. This method can be extended to other DNA binding proteins and enzymes, which have an affinity to mica higher than DNA, to improve sample preparation for AFM studies.

1. Introduction

A common application of biological atomic force microscopy (AFM) is molecular scale imaging of protein–nucleic acid interactions and has included studies of DNA transcription for the last twenty years or so [1–4]. Visualisation of molecular complexes through the force sensing AFM probe can be realised in hydrating air or aqueous liquids environments, depending upon the specific application, and whether or not the study is focussed mainly on structure or dynamics. Imaging of dried complexes in ambient air conditions can be termed *ex situ*, where the focus is investigating structural relationships between the protein and the DNA. Imaging of complexes *in situ* under aqueous buffers attempts to study dynamics in real-time or at least a time-lapse approach. Both of these two approaches requires the protein-DNA complexes to be adsorbed to a support surface, which is almost always mica, or mica which has been modified with a self-assembled monolayer or thin molecular film to promote binding of the DNA template [4,5]. Mica is an ideal support surface because it is atomically flat and its surface charge properties can be modulated using divalent cations to encourage DNA binding [6–9]. It should be noted that many studies indicate that the hydrophilic nature of the mica in typical ambient lab humidity keeps DNA hydrated [10–12].

Ex situ AFM imaging in air on mica has confirmed that *E. coli* RNA polymerase wraps the DNA template around itself during formation of the open promoter complex (RP_o) [13]. This effect has been quantified in detail by Rivetti et al. and can be used to establish the formation of RP_os in AFM imaging by measuring contour length reductions of linear DNA templates [14]. *In situ* imaging

* Corresponding author at: School of Physics and Astronomy, Woodhouse Lane, University of Leeds, LS2 9JT, UK.
E-mail address: n.h.thomson@leeds.ac.uk (N.H. Thomson).

http://dx.doi.org/10.1016/j.ymeth.2017.04.010
1046-2023/

has attempted to follow the process of transcription directly, but for the ground-breaking studies the scan speed of conventional AFM was too slow to capture more than a few frames [15,16]. This approach, however, imaged facilitated promoter location of *E. coli* RNAP on a linear template, demonstrating one-dimensional diffusion, hopping and inter-segmental transfer [17]. These were also the first imaging of the translocation of RNAP relative to DNA in the presence of NTPs, imaging transcription directly [15,16]. In one of the studies, the RNAP was bound stably to the mica surface and the DNA was free to move [15], but in different buffer conditions the RNAP was seen to move relative to the DNA, which was mobile but equilibrated onto the 2D surface of the mica [16]. Fine adjustment of buffer conditions is required for *in situ* experiments to allow the DNA sufficient movement for transcription to occur but restricting the DNA motion enough for the DNA backbone to be detected by the AFM tip [6–9].

More recently, the advent of higher scan speed AFMs has led to new attempts to follow transcription directly *in situ*. The major challenges of imaging DNA-dependent enzymes *in situ* by AFM arise from both the speed of the RNAP enzymes and the relative rotation of the DNA helix by a processive enzyme (such as RNAP). Higher frame rates partially address the first challenge and to address the second, these studies have tethered the DNA template strand by each end to a DNA origami nanotile as a way to overcome the conflicting requirements of DNA movement and localisation to the mica surface [18]. With this approach and frame rates of 1 image per second, promoter location and translocation of a single RNAP along the DNA template has been observed. Using real-time AFM imaging to analyse finer details of the transcription process may require further significant developments in the technology and methodology.

The *ex situ* approach can obviate, to a certain degree, these challenges: reactions are carried out *in vitro* and then the reaction can be quenched or run to completion and the outcomes imaged in a static manner [2]. DNA transcription is well suited to this approach, since RP_os can be pre-formed and are very stable before deposition onto a support surface. Once the RP_os are imaged, the NTPs can be added to the same *in vitro* reaction mix and incubated for a given period of time or quenched before the reaction mixture can be deposited and imaged again on mica [19].

The bacterial RNA polymerase from *E. coli* is the most widely studied by AFM, due to its relative simplicity and large size. This negates the need for additional factors, which might confuse interpretation of AFM images and gives confidence that the proportion of active complexes is high when NTPs are added. It is also noted that *E. coli RNAP* provides a model system for eukaryotic RNAPs due to the similarities in structure [20–23]. Our previous work on viral T7 RNAP showed that the *ex situ* AFM approach did not work particularly well because T7 RNAP spent the majority of the time off the DNA templates [24]. T7 is a fast and highly processive RNAP that re-initiates efficiently and is therefore able to perform multiple rounds of transcription *in vitro*. In our work, the probability of observing T7 RNAP on a DNA template by *ex situ* AFM was negligible. In the case of *E. coli* RNAP, it was generally expected that one enzyme will only perform one round of transcription, since the sigma factor sub-unit is not covalently attached to the holoenzyme and is expected to leave the complex shortly after or during initiation stages of elongation (also referred to as promoter escape). To date, however, the issue of sigma factor release has not been resolved with any degree of certainty [25–27]. This raises the uncertainty that *E. coli* RNAP may be able to perform multiple rounds of transcription complicating *ex situ* AFM analysis. Additionally, excess or free RNAP that has not formed an RP_o can non-specifically bind to the DNA template, other RNAP molecules and/or an RNA transcript leading to ambiguity in AFM images.

AFM studies of *E. coli* RNAP RP_o formation by Rivetti et al. and Crampton et al. have shown that there is shortening of the DNA contour length as well as a bend in the DNA giving a measurable angle of ~120°, which define this wrapping [13,14,19]. Even though these RP_os have a noticeably different appearance to non-specific interactions in *ex situ* AFM imaging, issues arise with the presence of other RNAP molecules attached to the DNA still undergoing their search for a promoter. Non-specifically bound RNAP can be confused for RP_os or active elongation complexes (ECs) [19]. There is therefore a need to inhibit this non-specific RNAP binding to optimise AFM analysis.

One of the simplest methods to reduce non-specific RNAP-DNA interactions is to increase salt concentration or ionic strength of the buffers used which leads to a decrease in the net electrostatic potential of the DNA. It is noted, however, that the rate of promoter binding decreases with increased salt concentration [28]. This change would mean that for *in vitro* transcription reactions to be analysed by AFM there would be a low number of RPOs for analysis. The effect of monovalent salts at high concentration can also alter the binding of the DNA and DNA-protein complexes to the mica surface and so may not be feasible for use in AFM [29–32]. This approach would also not solve the issue of multiple rounds of transcription occurring.

Biochemical methods overcome the issue of non-specifically bound RNAPs by the addition of the molecule heparin, which competes with DNA to bind RNAP in the DNA binding channel [33]. Heparin is a polyanionic polysaccharide of the glycosaminoglycan family (GAGs) which includes the closely related macromolecule heparan sulphate (HepS). Both heparin and HepS are linear polysaccharides made up of chemically similar monosaccharides but with varying degrees of sulphonation. Heparin is more highly sulphated than HepS, but HepS contains more N-acetylated monosaccharides. The exact chemical structure of any given heparin or HepS molecule can vary due to their non-templated production [34,35]. Both heparin and HepS are produced in the same manner and are made up of two repeating disaccharide units, the most common of which for each is shown in Fig. 1.

Heparin is produced by mast cells and has a molecular weight range of 60–100 kDa but when purified for biochemical uses has a size distribution of 12–15 kDa as purified from porcine intestine. HepS is produced by all cell types in the form of a proteoglycan, attached to a protein core. Free chains of HepS are rarely found *in vivo* but can be purified from bovine kidney cells free of the attached protein. The molecular weight of HepS has a similar range to that of heparin, but the average molecular weight of purified chains is slightly higher at approximately 20 kDa and it is less well characterised than heparin. The major biochemical difference between HepS and heparin is the number of GlcN-sulphate groups that occur. Both molecules have homologous structures and often are considered to display the same properties, and used as models of each other when necessary. Heparin and HepS chains adopt one of two right handed helical structures with a helical repeat of approximately 1.67 nm over a tetra saccharide sequence [36].

The use of heparin for *in vitro* transcription assays is a consequence of its comparable helical structure to DNA as well its polyanionic nature. Both DNA and heparin/HepS have a negatively charged backbone and adopt a helix with a residue rise of 0.4 nm for Heparin/HepS in comparison to 0.34 nm for DNA. Both are able to mimic DNA and bind to RNAP via its DNA binding domain located in the active site [33]. The similar structure of HepS means that it is also able to bind to DNA binding proteins in the same manner but is not commonly used due to its less well characterised chemical composition. The binding of heparin/HepS occludes the DNA from the active site thereby preventing the formation of RP_os. If an RNAP has already formed an RP_o, then heparin/HepS are unable to bind as they cannot gain access to the binding site

Please cite this article in press as: O. Chammas et al., Methods (2017), http://dx.doi.org/10.1016/j.ymeth.2017.04.010

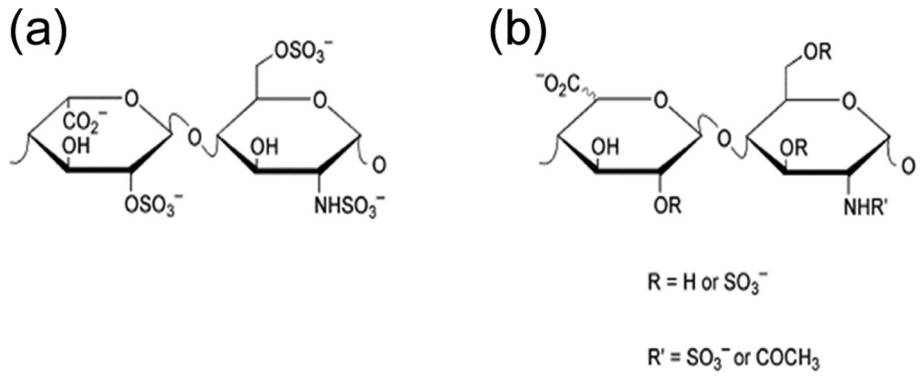

Fig. 1. Repeating disaccharide units that make up (a) heparin and (b) heparan sulphate. (a) For heparin, the most common disaccharide unit is composed of a 2-O-sulphated iduronic acid and 6-O-sulphated, N-sulphated glucosamine, IdoA(2S)-GlcNS(6S), making up >70% of the molecule. (b) For HepS, the most common disaccharide unit is composed of a glucuronic acid (GlcA) linked to *N*-acetylglucosamine (GlcNAc) typically making up around 50% of the total disaccharide units.

[33]. This means that heparin/HepS are able to bind free RNAP molecules that have not formed RP_os, non-specifically bound σRNAP, and RNAPs that have undergone elongation and are recycled for subsequent rounds of transcription [33,37,38]. This sequestering of free and non-specifically bound RNAPs has meant that heparin is used as a competitor for *in vitro* transcription reactions to ensure that only RNAPs that have formed RP_os, and therefore those that are actively transcribing, are being studied. The prevalent use of heparin as a competitor in biochemical assays suggests that heparin would be a good choice for AFM experiments, resolving non-specific binding events and preventing re-initiation and multiple rounds of transcription. However, addition of heparin or any of its derivatives into AFM samples has not been performed to date due to the potential risk of heparin interfering with the binding of DNA to the mica support surface, with researchers preferring to perform bulk biochemical assays only with heparin present [14].

Even though the use of heparin is standard for use in biochemical assays, it presents a potential significant problem for AFM samples. Heparin is believed to inhibit the binding of DNA to the mica support surface which is a reasonable assumption due to its highly anionic structure. The use of HepS instead of heparin has not been investigated to date but it is expected to exhibit similar effects, due to its similar structure and chemistry. HepS has a lower level of sulphonation as well a different chain length and so may interact with the mica surface in a different manner. As both are capable of inhibiting non-specific binding of RNAP both were considered in this study for incorporation into samples.

In recent times, more attempts are being made to investigate transcription on templates with more than one promoter by AFM and other techniques. These can be seen as simple *in vitro* models of gene structures that should give us greater insight into the basic underlying mechanisms involved in transcriptional interference (TI) [39–42]. Rivetti et al. have studied the formation of RP_os on DNA template comprising two tandemly oriented promoters [13]. While Mangiarotti et al. studied the formation of RP_os with two divergently orientated promoters inferring the effect that distance between the two promoters had on promoter occlusion [14]. Crampton et al. investigated a simple convergent gene model by *ex situ* AFM and observed the outcomes of RNAP-RNAP collisions. It was determined that head-on transcriptional interference between RNAPs occurred and that both "collisions" between an elongating RNAP and a sitting duck and those between two elongating RNAPs could occur [19].

In this study, we investigate the efficiency of RP_o formation on a linear DNA template with two tandemly oriented promoters which represents one of the simplest model of a gene. Here we present a study of the effects that the use of free heparin or heparan sulphate in solution has on the binding of the DNA alone, RNAP alone and the RP_os to a mica surface. We show that the use of either is viable in the presence of *E. coli* RNAP even though they can affect the adsorption of the DNA to the mica. We demonstrate that this is a consequence of the affinity of the *E. coli* RNAP for mica, showing that HepS is the most effective in use of *ex situ* AFM applied to DNA transcription.

2. Materials and methods

2.1. DNA template construction

The DNA template was generated from a 6136 bp pDSP plasmid (a kind gift from C. Rivetti) which contained two λ_{PR} promoters in a tandem arrangement using PCR. The two primers used were 5′ ATCTTCAACTGAAGCTTTAGAGCG 3′ (forward) and 5′ GTGTGAAATACCGCACAGATG 3′ (reverse) to define a DNA template of 1144 bp, with two promoters tandemly oriented (i.e. on the same strand pointing in the same direction) positioned at bases 435 and 773 from one end. PCR was carried out using GoTaq Hot Start Polymerase (Promega, Madison, WI) in 50 μL reactions and the template was purified using QIAquick PCR purification kit (Qiagen, Valencia, CA), both as per the manufacturer's instructions.

2.2. Open promoter complex formation

The given DNA template was mixed with *E. coli* σ^{70}RNAP (Epicentre, Madison MI) in 10 μL transcription buffer. The transcription buffer consisted of 20 mM Tris-HCl (pH 7.9), 50 mM KCl, 5 mM MgCl2, 1 mM DTT. The buffer used differed from that provided by the manufacturer, having no Triton X-100®. This was carried out in order to prevent any interference with the AFM sample preparation and analysis but still enable the protein to perform its function.

The amount of DNA used in the reaction was 200 fmol. The amount of RNAP used was based on a 1:1 ratio of promoters on the DNA template to RNAP, i.e. 400 fmol of RNAP, as this was shown to provide the highest yield of RP_os observed by AFM, while limiting the levels of non-specific interactions of RNAP with a given DNA template in the absence of polysaccharide [19]. The activity of RNAP was assumed to be 100%. RNAP was stored at −80 °C in small aliquots to ensure repeat freeze thaw cycles did not occur. Once the samples had been mixed by gently pipetting up and down they were incubated at 37 °C for 20 min in order to allow RP_os to form.

Once incubated, samples were diluted by a factor of 10 in imaging buffer before being deposited and dried for AFM analysis.

2.3. Introduction of heparin or heparan sulphate

The protocol used in this study was partly based on that used by Rivetti et al. [13]. They pre-incubated RNAP with 70 μg/ml of heparin and mixed 40 fmol of pre-incubated RNAP with 10 fmol of DNA template with a single PR promoter DNA template before depositing the samples in a deposition buffer containing a further 70 μg of heparin. It is important to note that this preparation was to establish a control sample to demonstrate that non-specific RNAP binding to the DNA template did not produce reduction of the DNA contour length, in contrast to RP_o formation. For *in vitro* transcription Rivetti et al. used 200 μg/ml heparin in RP_o samples containing 600 fmol of RNAP holoenzyme in transcription buffer to ensure heparin was in molar excess, however, these samples were not studied by AFM [6].

In this study, heparin or HepS was added to 10 μL of transcription buffer at final concentration of 200 μg/ml or 1000 μg/ml before being diluted 1 in 10 in imaging buffer. This was then deposited onto mica and incubated for 3 min, rinsed with dH_2O and dried with nitrogen before imaging.

To study the effects of heparin and HepS on the binding of DNA to mica, 200 fmol of DNA was added to 10 μL of transcription buffer with heparin or HepS at final concentration of either 200 μg/ml or 1000 μg/ml. These were then prepared for imaging as in previous samples.

To study the effects of heparin or HepS on RNAP and its absorption to the mica surface, samples were prepared containing 400 fmol of RNAP holoenzyme and 200 μg/ml of heparin or HepS in 10 μL transcription buffer. These were diluted 1 in 10 in imaging buffer before being deposited and dried for imaging.

To study the effects of heparin and HepS on the formation of RP_o, RP_os were formed as described above and then straight after removal from incubation at 37 °C, heparin or HepS from bovine kidney (Sigma, Saint Louis, MO) with an average molecular weight of 20 kDa was added to a final concentration of 200 μg/ml and the sample was incubated at room temperature for 15 min.

2.4. AFM sample preparation

Once molecular samples with and without a polysaccharide had been formed, 1 μL of the sample was diluted into 9 μL of imaging buffer: Tris-HCl (4 mM, pH 7.5), 4 mM $MgCl_2$. The full 10 μL of sample in imaging buffer was deposited onto freshly cleaved muscovite mica (Agar scientific, Essex UK) and incubated on the surface for 5 min to ensure that complexes adsorbed to the mica surface.

After incubation, samples were rinsed using with 5–8 ml ultrapure water with a resistivity of 18.2 MΩ·cm (at 25 °C). The mica disc was held with tweezers freshly cleaned with ethanol and tilted to prevent pooling of water on the surface. The water was exuded at a flow of approximately 0.5–1 ml per second to ensure removal of any molecules loosely bound to the mica. Once a sample was rinsed, it was dried in steady stream of nitrogen at 1 bar of pressure until all liquid was removed from the surface. Once the sample was dried it was stored in a standard petri dish at ambient lab humidity (30–40%) and imaged within 24 h

2.5. Atomic force microscopy

AFM imaging was performed using a FastScan Bio AFM (Bruker, Billerica MA) using Fastscan A cantilevers (Bruker, Camarillo CA). The specification of the FastScan A cantilevers used are given in Table 1. The AFM was operated in tapping mode in air at room temperature (22–25 °C).

Table 1
Summary of the Fastscan A cantilever specifications used for the AFM imaging.

	Fastscan A
Material	Silicon nitride
Cantilever geometry	Triangular
Thickness (nominal)	0.58 μm
Back side coating	Reflective aluminum
Tip radius (nominal)	12 nm

The cantilever auto tune function was used to locate the resonant frequency for each cantilever probe and the frequency of oscillation was offset by a maximum of 5% below the resonance. The offset was used to ensure that the cantilever operated in standard tapping mode. The amplitude of oscillation was initially set to 500 mV and the set point was initially selected automatically. These were altered from sample to sample and throughout imaging along with the integral and proportional gains to provide the best image quality. Images were collected using between 512 and 1024 samples per line at a line scan rates ranging from 11 to 22.4 Hz but this was changed depending on the sample tip interactions and image quality on the day. The standard parameter ranges for operation of the AFM is given in Table 2. All images were collected using a Z-range of 5 nm unless otherwise stated. The higher scanning speed of the Bruker FastScan Bio AFM allowed sample survey imaging to be carried out at multiple points across the sample. Samples were surveyed by taking between 5 and 18 images of each using scan sizes of between 2 × 2 and 5 × 5 microns per image.

2.6. AFM image analysis

2.6.1. Image processing

The raw AFM image files were exported to the AFM manufacturer's software Nanoscope Analysis 1.4 or 1.5 (Bruker, Billerica MA). The files were then flattened in the 0th order to centre the data in the digital Z range and subsequently flattened in the 3rd order to remove tilt and bow. Flattening utilises a best fit polynomial fit for each line of data to centre data (0th order) or remove tilt and bow (3rd order). After flattening, for all images the Z-range (height) was set to 5 nm and for phase images the data scale used was 10°.

2.6.2. Molecular counting

Molecules of RNAP were counted using the particle detect feature of the Nanoscope software. This feature detects particles by using the pixel height over a given height threshold, set at 2 nm to distinguish them from the mica background. An upper limit of 35 nm for diameter was used to define a single RNAP, which is the typical size of the *E. coli* RNAP when imaged using tapping mode AFM in air with a standard tip. Any particles above the threshold of 35 nm diameter were determined to be aggregates of RNAP. Particles that were not automatically detected correctly by the software, such as two RNAP in close proximity that were not touching, were manually added or discounted as necessary.

Table 2
Typical operating parameters of the tapping mode AFM in this study.

	Fastscan
Setpoint	500–1500 mV
Integral gain	1.0
Proportional gain	5.0
Scan rate	11.0–22.4 Hz
Samples per line	512–1024
Amplitude of oscillation	2–20 nm

2.6.3. DNA contour length measurements

In order to perform DNA contour length measurements, files were exported as JPEG or BMP files which maintained the pixel ratio of the original image before being loaded into the analysis suite ImageJ [43]. DNA contour length measurements were performed by manually tracing a line along the DNA backbone. When RNAP was bound to the DNA, the contour length was measured to the centre of the RNAP molecule, as judged by eye, in the 2D representation of the AFM image. Lengths were recorded and plotted in histograms using OriginPro with an n value of 100 molecules or greater. Histogram bin size number was set from the data range divided by the square root of n. Errors for length measurements are given as the standard error of the mean value.

Fitting of the peak values was performed using the OriginPro fitting Gaussian fitting function with the y value set zero where possible. For single peaks the equation used was:

$$y = y_0 + \frac{A}{w\sqrt{\pi}/2} e^{-2\frac{(x-x_c)^2}{w^2}}$$

The parameters used were area (A), offset (y_0), centre (x_c) and width (w). Derived parameters were the full width half maxima, standard deviation and height of the curve fit.

3. Results

3.1. Heparin and heparan sulphate binding to mica

Heparin or HepS have never been used directly within AFM samples to study transcription due to a reasonable hypothesis that the highly negative charge of polysaccharide chains will compete with or prevent binding of the DNA to the mica surface. Rivetti et al. utilised heparin in samples for investigations into the wrapping of DNA by *E. coli* RNAP upon formation of RP_os [13]. In that study, heparin was pre-incubated with the RNAP such that RP_os would not form and only non-specifically bound RNAP was present on the DNA template. This was to establish that DNA contour length reduction was only due to wrapping of the DNA around the RNAP upon RP_o formation and not due to any other non-specific RNAP binding. In a later study on promoter interference, it was stated that "heparin could not be used in the AFM experiments because it prevents adhesion of the DNA to mica", but no data were provided to demonstrate this effect [14].

In order to provide a full picture of the effects that heparin or HepS may have on AFM analysis of transcription complexes, first control samples of only heparin or HepS were studied. The two concentrations of the polysaccharides used for RP_o formation *in vitro* were the typical value of 200 μg/ml and a high concentration of 1000 μg/ml, chosen arbitrarily to study how it may influence binding of DNA to mica. Both polysaccharides were dispersed well over the surface, but HepS had a tendency to show more aggregates, particularly at the higher concentration (Fig. 2). It can be seen, particularly from the AFM tapping mode phase images, that the appearance of the surface with the addition of heparin or HepS is different. It appears that in both cases the polymers form a continuous thin film on the mica with individual molecules or small aggregates lying on top.

The difference in appearance between double-stranded DNA and heparin or HepS molecules is due mainly to the different flexibility of these polymers. DNA is a semi-flexible polymer that can be modelled reliably using the worm-like chain model with a persistence length of ~50 nm [44], whereas heparin and HepS with a single backbone, are highly flexible and heparin has been modelled as a freely-jointed chain with flexibility on the length scale of the individual sugar rings based on AFM force extension measurements [45], although SAXS and hydrodynamic methods indicated that heparin might be stiffer, fitting a worm-like chain with a persistence length of ~4.5 nm [46].

3.2. Heparin and heparan sulphate with DNA

Next the influence of heparin and HepS on the binding of DNA to mica was investigated by first mixing the two concentrations of each with the DNA solution at the standard concentration used for *in vitro* transcription reactions, before co-deposition on the mica. These samples displayed a variety of different morphologies in the AFM images (Figs. 3–6), but typically dsDNA was not visible as semi-flexible individual molecules as is the case in the absence of the polysaccharide polymers (Fig. 3e).

The surface density of DNA detected by the AFM varied substantially across the surface. Some regions were found on both the heparin and HepS samples where individual DNA molecules were resolved and qualitatively exhibited the semi-flexible polymer like appearance (Figs. 3–5). Interestingly, for these areas of the sample, the surface density of the DNA bound to the mica was augmented by the presence of the polysaccharide at the higher concentration of 1000 μg/ml, with heparin having a greater effect than HepS (Fig. 3). Even so the appearance of the DNA molecules differed from images of DNA deposited alone (see Fig. 3e) and the lower AFM image contrast compared to DNA deposited alone implies that polysaccharide material is co-deposited with the DNA.

In other areas, the use of the tapping mode phase signal revealed more clearly that the polysaccharide is bound in and around the DNA. This is exemplified at the lower polysaccharide concentration where the molecular surface density is lower (Fig. 4). It also tends to imply an interaction between the polysaccharides and DNA.

In general, regions where individual DNA molecules were clearly visible were not very commonplace and in other regions of the samples the polysaccharide appeared to compete with the DNA for binding to the mica as expected. Co-deposition of polysaccharide and the DNA was more clearly evident at higher polysaccharide concentrations, where in other regions individual DNA molecules could be observed within a thin film of material where the morphology for heparin and HepS was somewhat different (Fig. 5). These layers were often not stable and moved under the presence of the scanning AFM tip (see Fig. 5b), implying that molecules in the surface of the thin film were not securely attached to the surface. Fig. 5 demonstrates that DNA can bind within the surface layer in the presence of the polysaccharide, or resides on the surface of the thin film, but that binding of heparin or HepS tends to dominate.

Most typically, the AFM survey imaging of the surface showed regions where DNA molecules were not observed or detected by the AFM tip (Fig. 6). For the lower polysaccharide concentration, the appearance was that of a continuous thin molecular film across the mica and in places this was disrupted (Fig. 6a left) demonstrating coverage of the surface. In many areas for the higher concentrations, aggregates were imaged that ranged in size up to 500 nm across, but there also appeared to be a continuous underlying thin film as well. The aggregation is possibly a consequence of molecular condensation during the drying process caused by de-wetting instability of a thin film of DNA + polysaccharide physisorbed onto the mica. These two typical morphologies of continuous thin film and regions of aggregation were randomly dispersed over the surface of the mica but the aggregates were much more prevalent at the atypically high polysaccharide concentration of 1000 μg/ml.

Taken all together, the sample survey imaging of the polysaccharide + DNA samples inferred the interpretation that a densely packed thin film containing both types of molecules is formed on the mica surface. It is presumed to be a network of DNA and

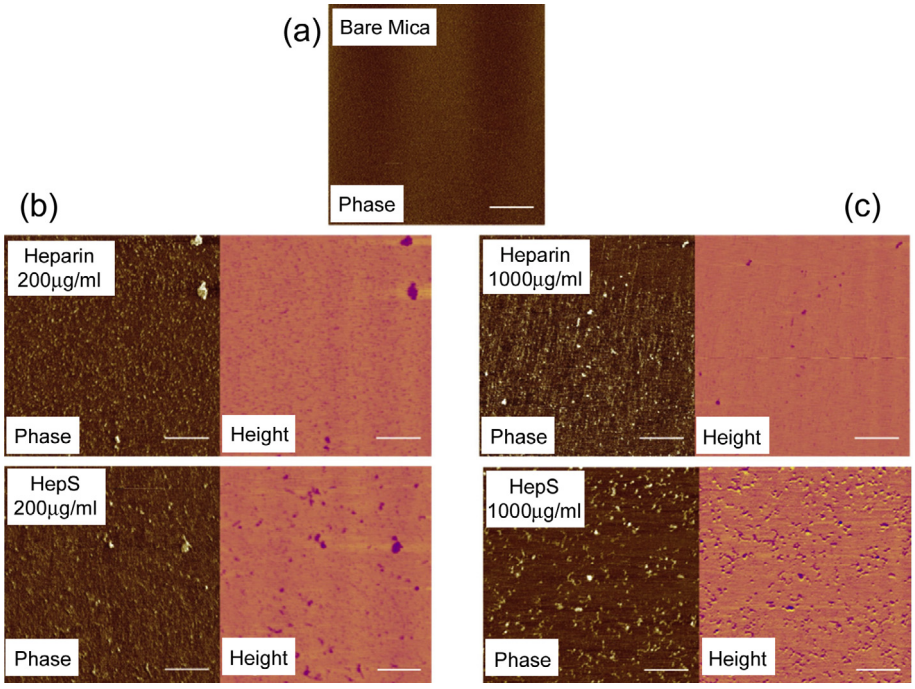

Fig. 2. AFM tapping mode phase and height images of heparin and HepS deposited on mica. (a) The control: AFM phase image of freshly cleaved mica. (b) Heparin and HepS deposited at 200 μg/ml. (c) Heparin and HepS deposited at 1000 μg/ml (Scale bars: 200 nm).

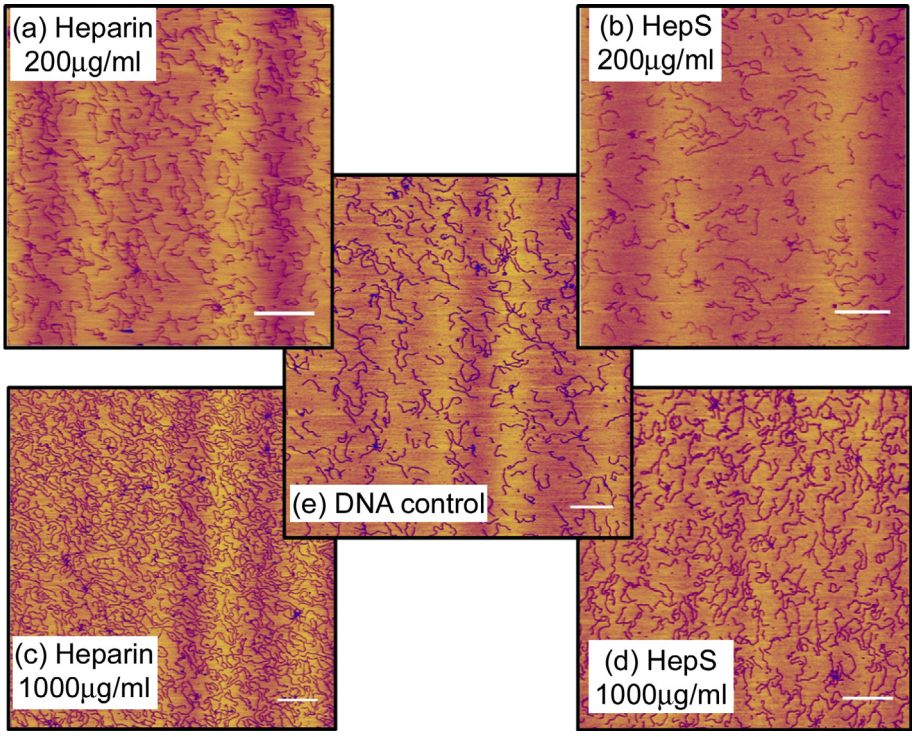

Fig. 3. AFM height images of regions of 1144 bp DNA template co-deposited with heparin or HepS at the two chosen *in vitro* concentrations (a, b, c, d). In these regions, individual DNA molecules are resolved by the AFM tip and the polysaccharide at 1000 μg/ml can augment the DNA surface density. (e) A control sample of DNA alone deposited at the same DNA concentration without polysaccharide molecules (Scale bars: 500 nm).

heparin or HepS together, since DNA molecules can be resolved in certain regions. It is not possible to say whether the aggregates contain only DNA but it might be expected that these are likely to be condensates of DNA + polysaccharide, mediated by the Mg^{2+} ions available in solution. Overall, one can say that it is not possible to reliably image individual DNA molecules in the presence of heparin or HepS at concentrations typically used for *in vitro* transcription reactions.

Please cite this article in press as: O. Chammas et al., Methods (2017), http://dx.doi.org/10.1016/j.ymeth.2017.04.010

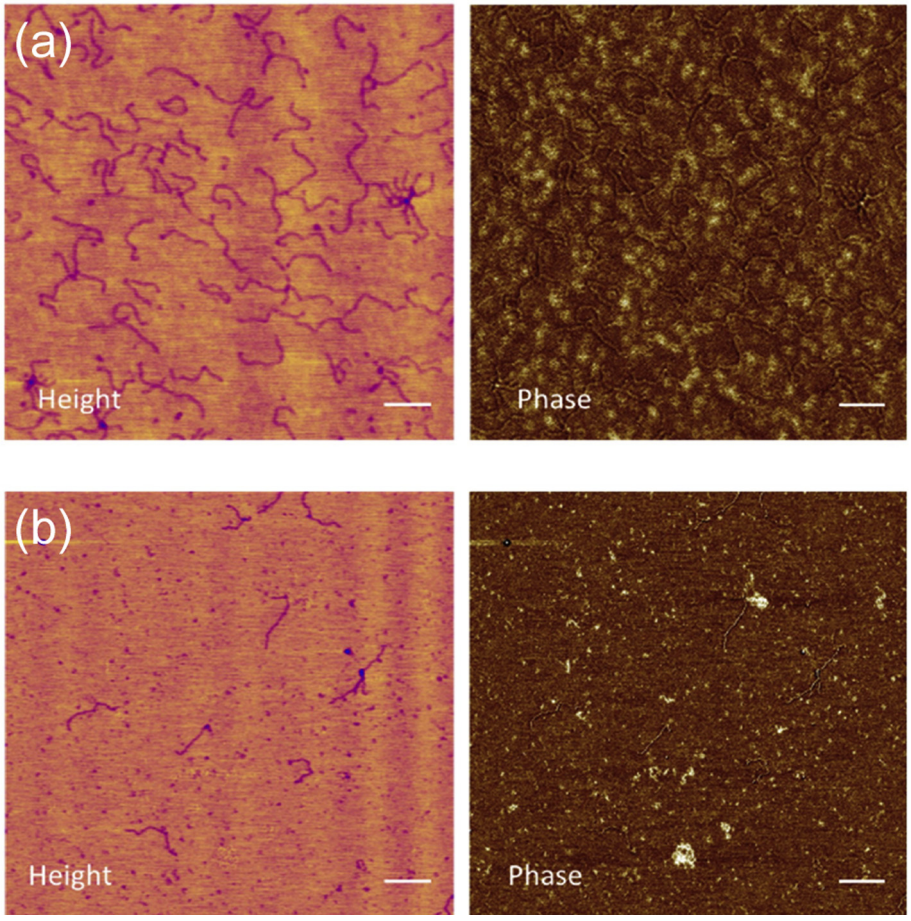

Fig. 4. AFM height and phase images of regions of the 1144 bp DNA template co-deposited with (a) heparin or (b) HepS both at 200 μg/ml concentrations. Individual DNA molecules were visible on the mica but not as clear as typical images of DNA deposited alone. It can be seen from the phase images (right column) that for both (a) heparin and (b) HepS containing samples, the DNA has polysaccharide material bound to the mica surface around and/or underneath the DNA (Scale bars: 200 nm).

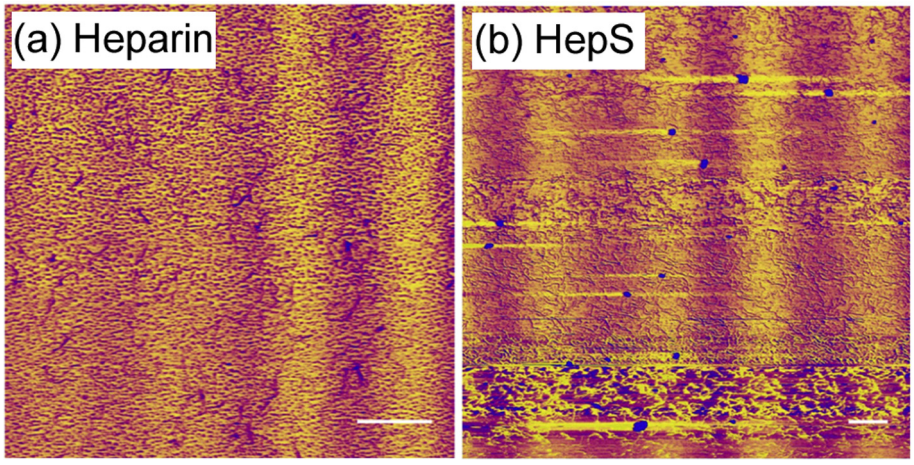

Fig. 5. AFM height images of DNA co-deposited with (a) heparin or (b) HepS on mica at 1000 μg/ml concentration where individual DNA molecules of the 1144 bp DNA template within a close packed layer can be seen. The surface structure was often disturbed by the scanning AFM tip, particularly in the case of HepS (Scale bars: 500 nm).

3.3. Heparin and heparan sulphate with RNAP holoenzyme

Next, the effect of heparin and HepS on adsorption of *E. coli* RNAP holoenzyme alone was tested. Since both concentrations of either polysaccharide were detrimental to the binding of DNA alone to mica, the experiments in the presence of RNAP, either alone or as RPo (see Section 3.4), were conducted with the typical *in vitro* concentration of 200 μg/ml. In contrast to the DNA samples, the distribution of RNAP on mica in the presence of the polysaccharides was homogeneous, however, some protein aggregation was observed. Fig. 7 shows typical examples of the holoenzyme dispersed on mica in the absence and presence of the polysaccharides. The protein spontaneously adsorbs to mica but can form some small aggregates. The total amount of protein bound to the mica

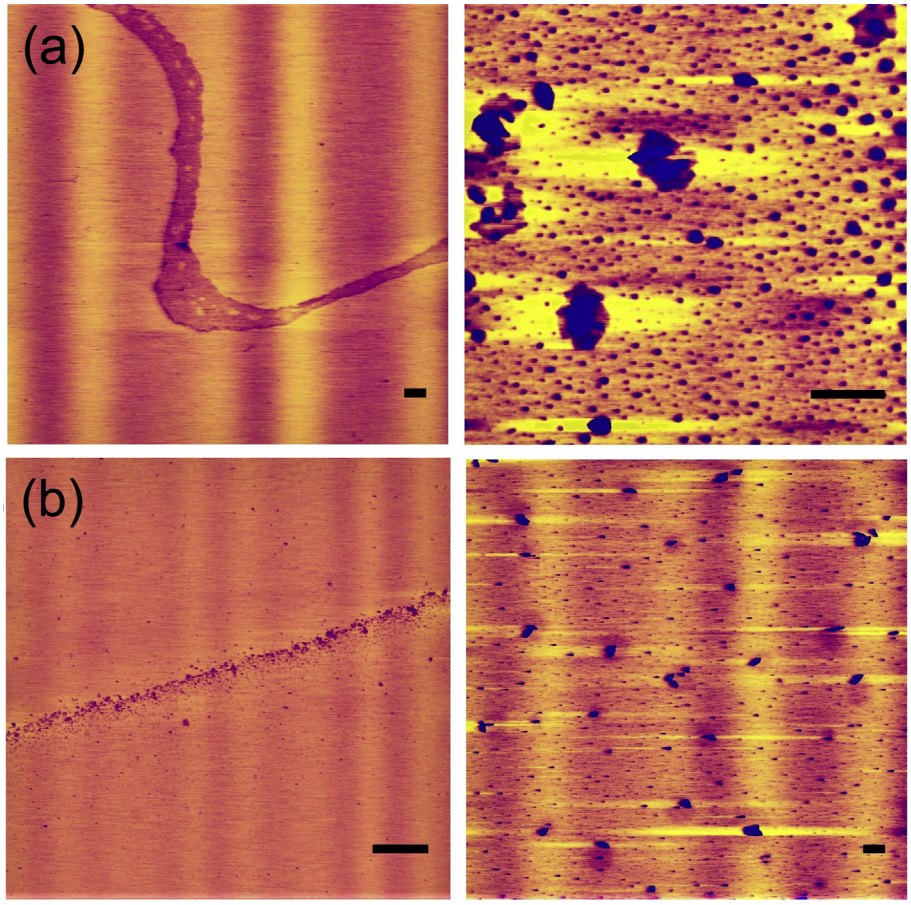

Fig. 6. AFM height images of some typical structures formed by co-deposition of (a) DNA with the polysaccharide heparin or (b) DNA and HepS onto mica. The images in the left column were taken with a polysaccharide concentration of 200 μg/ml while for the images in the right column, the concentration of heparin or HepS was 1000 μg/ml (Scale bars: 500 nm).

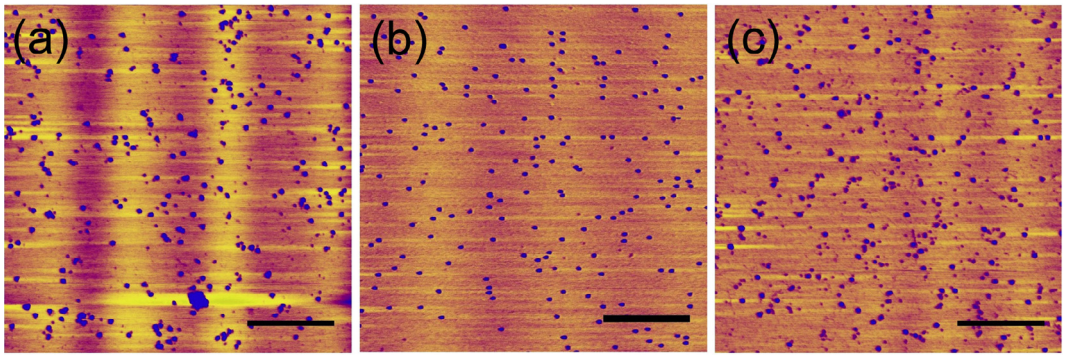

Fig. 7. Typical images of *E. coli* RNAP holoenzyme deposited on mica and imaged in air. (a) Control with no polysaccharide present, (b) with heparin and (c) with HepS both at 200 μg/ml concentration (Scale Bars: 500 nm).

was similar in each case, but the number and size of the aggregates varied. The number of singular RNAPs and small aggregates for each sample type are shown in Table 3. The aggregation state of the RNAP was more pronounced in the control with neither polysaccharide added (Fig. 7a), where aggregates were more numerous and overall larger, limiting the number of single RNAPs observed. The addition of either heparin or HepS decreased the size and number of aggregates of RNAP and led to greater dispersion of single RNAPs across the mica surface. In the absence of the polysaccharide binding competitor, the proportion of aggregates in the images was ~20%, whereas in their presence this dropped to below 5%. In general, the monodispersity of RNAP in the presence of heparin looked the best (Fig. 7b) but the yield of single RNAP on the mica surface was similar for both heparin and HepS, based on the criterion of an individual RNAP being 35 nm in diameter.

In summary, the binding of RNAP to the surface is not inhibited by either heparin or HepS, but the dispersion of individual RNAP across the mica surface is increased by the presence of the polyanionic polysaccharide molecules. In general, this indicates that binding of the polysaccharide to the RNAP reduces unwanted RNAP-RNAP interactions. This could be a consequence of two effects;

Please cite this article in press as: O. Chammas et al., Methods (2017), http://dx.doi.org/10.1016/j.ymeth.2017.04.010

Table 3
Number of RNAPs bound to the surface as singular RNAPs or aggregates in the presence of heparin or HepS. The number of RNAPs in five 2 μm^2 images was counted for each sample.

Sample	n (number of images)	Single RNAP molecules	Aggregated RNAPs
Control	5	159 ± 20	42 ± 4
Heparin	5	516 ± 26	26 ± 4
HepS	5	557 ± 53	26 ± 4

firstly because the polysaccharide bound in the DNA binding pocket changes the conformation of the RNAP, and secondly because the polysaccharide may wrap itself around the outside of the protein and change its surface charge characteristics. Importantly, there was no evidence that the polysaccharides bound to the mica surface in the presence of RNAP, in contrast to the DNA samples, giving confidence that heparin or HepS can be used in transcription samples for *ex situ* AFM imaging.

3.4. Formation of open promoter complexes on the tandem DNA template

As RNAP was seen to be able to bind to the mica in the presence of heparin and HepS, their effect on DNA-RNAP complexes was investigated. In order to provide comparison to the previous experiments performed by Rivetti et al. and Crampton et al. without heparin or HepS present, open promoter complexes (RP_os) were formed and then heparin or HepS was added to a final concentration of 200 μg/ml. In these experiments, we used a 1144 bp DNA template with two promoters tandemly oriented (i.e. on the same strand pointing in the same direction) positioned at bases 435 and 773 from one end. RP_os can be identified through DNA contour length measurements due to the shortening of the DNA template due to *E. coli* RNAP wrapping DNA upon RP_o formation [13,14,19]. This allows one to identify specific RP_os and exclude those where RNAP is not bound in the correct position or bound with more than two RNAPs.

Fig. 8 shows typical survey AFM images (fields of view) for samples without (a) any polysaccharide present, (b) heparin present and (c) HepS present. Upon addition of heparin or HepS there is an increase in bare DNA in comparison to samples without either heparin or HepS. This is expected as both these RNAP binders reducing non-specific interaction of RNAP with DNA, sequestering free RNAP that has not bound and formed an RP_o. The addition of both heparin and HepS reduces the level of non-specific binding observed. It was also noted that when heparin or HepS was present, any remaining non-specific binding was mainly limited to the ends of the template, whereas without either inhibitor a number of aggregated complexes were seen.

The percentage of molecules with a single RP_o formed, two RP_os formed and non-specifically bound RNAPs bound were determined by measuring the full DNA contour length and counted (see Table 4). Those complexes with just non-specifically bound RNAP give a contour length in good agreement with bare DNA. Formation of only one RP_o on one of the promoters gives a decrease in overall contour length due to DNA wrapping around the RNAP of ~25 nm, while double RP_os with both promoters occupied show a decrease of ~50 nm (Fig. 9). Both polysaccharides lower non-specifically bound RNAP by up to three fold. Heparin doubles the amount of single RP_os compared to the control, but interestingly does not enhance the proportion of double RP_os significantly. HepS on the other hand, maximises the yield of double RP_os on this tandem promoter template such that they become the major species of RNAP-DNA complexes as visualised by AFM. This is ideal for studying transcription of templates with more than one promoter by AFM and demonstrates that HepS is a better choice than heparin as a competitive binding inhibitor of free RNAP for *ex situ* AFM. This will enable analysis of transcription at the single molecule level to be carried out with greater rigour with particular focus on the outcomes of multiple RNAP acting on single DNA templates.

4. Discussion

Introduction of a polysaccharide competitive binding inhibitor changes the conformation and/or surface properties of the RNAP and enhances its dispersion on mica. Apparently, neither heparin nor HepS are retained on the mica surface when samples are made with just RNAP plus polysaccharide binding inhibitor. The stronger binding of RNAP to mica compared to the DNA template enables heparin or HepS to be used to enhance yields of RP_os for transcriptional analysis by *ex situ* AFM. Both heparin and HepS disperse the samples more effectively on the mica by reducing unwanted RNAP-RNAP interactions, as well as unwanted RNAP-DNA interactions. HepS is more effective at increasing the yield of double RP_os on a template with two promoters. We therefore determine HepS to be our preferred RNAP binding inhibitor for our system, which will define single cycle transcription to make *ex situ* AFM analysis more rigorous.

Both polysaccharides are seen to compete with DNA to bind to the mica surface, which is confirmation of an effect which led to heparin not typically being previously considered or used in AFM experiments of transcription [13,14,19]. The efficacy of this new approach works because *E. coli* RNAP has the highest binding affinity to mica of all the molecular components. It is interesting that previously Mangiarotti et al. found that addition of heparin into the RP_o mixture was incompatible with AFM sample preparation [14]. There are very slight differences between their AFM sample deposition buffer and ours, which might affect the affinity of the RNAP to the mica. Theirs was a HEPES buffer which contained 10 mM NaCl [14], whereas ours is a Tris-HCl and contained no additional monovalent salt, such as sodium chloride [19].

It is expected that our approach can be extended to other RNAPs or DNA binding proteins for AFM analysis, provided that the protein has a good affinity for the mica under the buffer conditions used. When RNAP is present, either alone or with the DNA template, the polysaccharide molecules are not retained on the mica during the rinsing step and therefore do not interfere with image analysis. Any that are retained are presumably bound to any RNAP that has not formed an RP_o.

Interaction of the polysaccharides with DNA alone is complicated, but in general there are interactions between these molecules and the mica which lead to a thin film of material that contains both DNA and polysaccharide. The survey imaging of the surface suggests that the DNA and polysaccharide may phase segregate to a certain degree into different regions containing different relative amounts of each molecule. Overall, it indicates that the polysaccharide has a higher affinity for the mica than this DNA template but this effect is obviated in the presence of RNAP.

One proposed method to circumvent the problem of non-specific RNAP binding is to use heparin attached to another substrate during sample preparation to try to purify RP_os from free and non-specifically bound RNAP. A method by Ebenstein et al. to study transcription involved the use of heparin attached to sepharose beads which were subsequently centrifuged down into a pellet after addition to a sample leaving only RNAPs in RP_os in the supernatant [319]. This method has a potential advantage over the use of free heparin, the fact that any heparin bound RNAPs are removed from the sample, and therefore is expected to increase the yield of RP_os for imaging and statistical analysis.

Even though this method would remove any non-specifically bound RNAPs after formation of RP_os, it would not prevent re-initiation events due to the lack of a competitor in the reaction

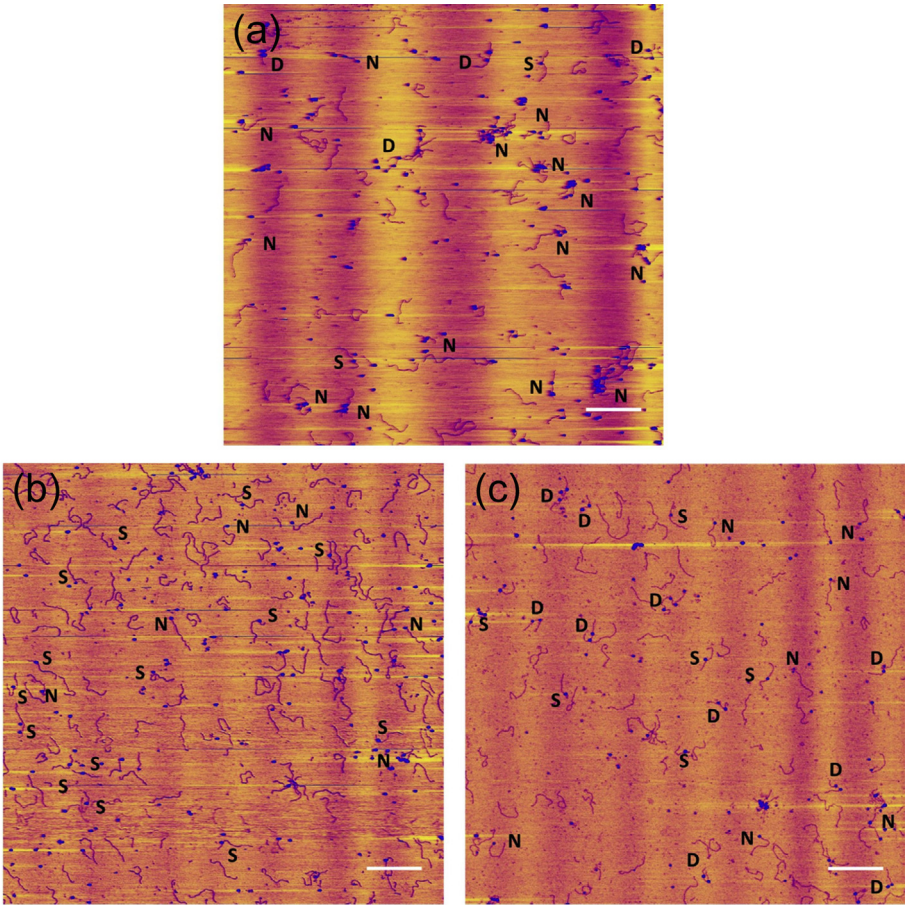

Fig. 8. AFM height images of RP_os formed on the tandem promoter 1144 bp DNA template (a) without any inhibitor and (b) with heparin or (c) with HepS. The images have been annotated with an S to signify those with single RP_os, a D to signify those with two RP_os and an N to signify those that have non-specifically bound RNAP (Scale bars: 500 nm).

Table 4
Percentages of complexes formed without a polysaccharide binding inhibitor and with heparin or HepS. The contour lengths of the 1144 bp DNA molecules are also given in parentheses with single RP_os showing a decrease in contour length of approximately 25 nm, double RP_os a decrease of approximately 50 nm and the non-specifically bound DNA showing no decease compared to the bare DNA control.

Sample	Single RP_o (nm)	Double RP_os (nm)	Non-specifically bound RNAP (nm)
−heparin/−HepS (n = 236)	30% (356.4 ± 1.5)	17% (331.4 ± 1.8)	53% (382.9 ± 1.3)
+heparin (n = 200)	60% (350.2 ± 1.4)	22% (328.5 ± 1.8)	17% (379.4 ± 6.5)
+HepS (n = 233)	33% (358.4 ± 1.0)	51% (328.3 ± 0.9)	14% (379.5 ± 2.9)
Bare DNA (n = 102)		380.16 ± 1.2	

during and post transcription initiation. We carried out some systematic experiments with heparin sepharose (HS) beads and found that although it removed free unbound RNAP from the reaction mix it also reduced the solution concentration of RP_os and free DNA (Data not shown). This was true for all concentrations of HS beads tested relative to the RNAP and DNA concentrations and was independent of bead incubation time in the reaction mixture or whether or not the beads were centrifuged for sedimentation. The efficacy of the centrifugation based method with HS beads was also investigated and compared with the free heparin or HepS approach. Contrary to expectation, the HS bead method did not improve RP_o yield under our conditions and moreover we show that the centrifugation of the samples in the presence of the beads can be detrimental to the sample preparation lowering overall yields of all molecular species. We concluded, therefore, that the HS beads are less suitable than adding free polysaccharide as a way to enhance analysis of *in vitro* model transcription complexes for analysis by *ex situ* AFM.

In summary, therefore, we find that addition of an RNAP binding inhibitor free in solution sequesters unbound RNAP after RP_o formation such that RNAP cannot re-bind to the DNA template. This approach will ensure that any given *E. coli* RNAP only carries out a single cycle transcription in the reaction mix thereby preventing unwanted binding or re-binding skewing statistical analysis of RNAP positions. This is important for *ex situ* AFM since multiple rounds of transcription cause asynchronicity in the system, which may lead to mis-interpretation of the outcomes from this type of snap-shot analysis based on the morphological detection of RNAP in the AFM images. We are currently re-considering the outcomes of our work concerning RNAP-RNAP collisions events in a convergent model gene system using *ex situ* AFM [19] in light of our ability to now define single cycle transcription. This method could in principle aid *in situ* AFM used to observe transcription directly, however there are on-going issues of time-resolution and activity that need to be resolved, such that we currently favour the *ex situ* approach for studying and analysing transcription by AFM.

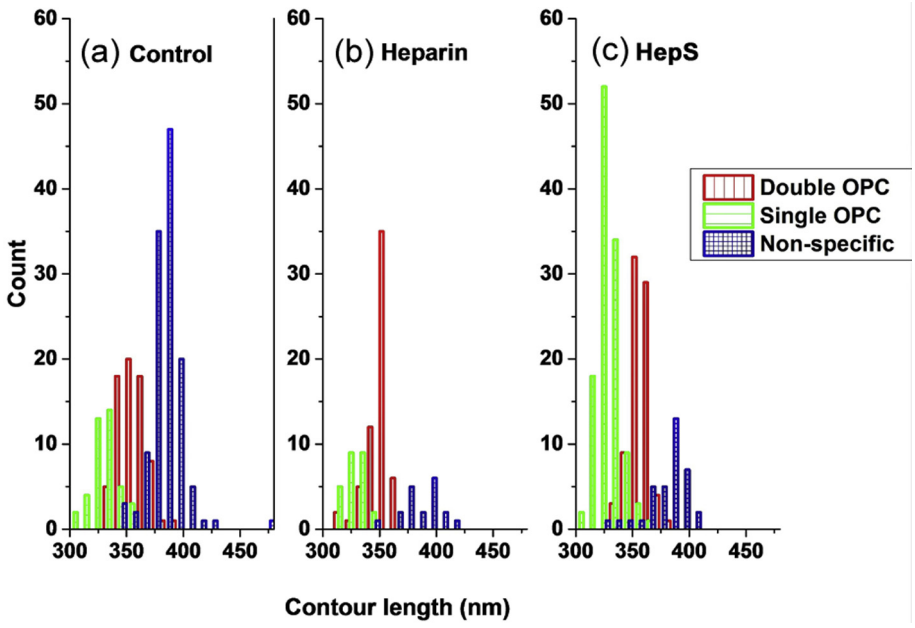

Fig. 9. Contour length histograms for the DNA molecules for non-specific RNAP binding (blue), single RP_o formation (red) and double RP_o formation (green). (a) Control with no polysaccharide, (b) incubated with heparin, (c) incubated with HepS both at 200 μg/ml concentration. (For interpretation of the references to colour in this figure legend, the reader is referred to the web version of this article.)

5. Conclusions

We have demonstrated that polysaccharide binding inhibitors of *E. coli* RNAP can be used very effectively to increase the yield of RP_o formation for AFM analysis, contrary to previous expectations. Heparan sulphate, which has previously not been tested, was more effective than heparin, particularly for increasing yields of double RP_os on the tandem promoter template. The overall effectiveness of this approach lies on the increased affinity of RNAP for mica in the presence of a polysaccharide binding inhibitor, as well as lack of retention of free polysaccharide on the surface in the presence of RNAP. This new method will be particularly important for *in vitro* study of simple model gene structures using *ex situ* AFM, which contain more than one promoter. It could be extended for other RNAPs or DNA binding proteins for AFM analysis, provided that the protein in question has a high enough affinity for the mica support surface. Where this is not the case, the mica surface properties can be modulated either by ion-exchange or formation of a surface film, such as poly-L-lysine or aminosilane, to encourage any particular protein to bind. We therefore believe this a powerful new approach for studying DNA-binding proteins at molecular resolution with AFM.

Acknowledgements

OC was funded through the EPSRC Centre for Doctoral Training in Molecular Scale Engineering (EP/J500124/1). We thank Vanessa Woodhouse for her contribution to the heparin sepharose bead study. The data used within this publication is available at http://doi.org/10.5518/145.

References

[1] A. Alessandrini, P. Facci, AFM: a versatile tool in biophysics, Meas. Sci. Technol. 16 (2005) R65.
[2] D.J. Billingsley et al., Single-molecule studies of DNA transcription using atomic force microscopy, Phys. Biol. 9 (2012) 021001.
[3] F. Wang, E.C. Greene, Single-molecule studies of transcription: from one RNA polymerase at a time to the gene expression profile of a cell, J. Mol. Biol. 412 (2011) 814–831.
[4] Y.L. Lyubchenko, L.S. Shlyakhtenko, Imaging of DNA and protein–DNA complexes with atomic force microscopy, Crit. Rev. Eukaryot. Gene Expr. 26 (2016) 63–96.
[5] H.K. Christenson, N.H. Thomson, The nature of the air-cleaved mica surface, Surf. Sci. Rep. 71 (2016) 367–390.
[6] H.G. Hansma, D.E. Laney, DNA binding to mica correlates with cationic radius: assay by atomic force microscopy, Biophys. J. 70 (1996) 1933–1939.
[7] N.H. Thomson et al., Reversible binding of DNA to mica for AFM imaging, Langmuir 12 (1996) 5905–5908.
[8] D. Pastre et al., Anionic polyelectrolyte adsorption on mica mediated by multivalent cations: a solution to DNA imaging by atomic force microscopy under high ionic strengths, Langmuir 22 (2006) 6651–6660.
[9] D. Pastre et al., Adsorption of DNA to mica mediated by divalent counterions: a theoretical and experimental study, Biophys. J. 85 (2003) 2507–2518.
[10] N.H. Thomson, Imaging the sub-structure of antibodies with tapping-mode AFM in air: the importance of a water layer on mica, J. Microsc. 217 (2005) 193–199.
[11] D.J. Billingsley et al., Atomic force microscopy at high humidity: irreversible conformational switching of supercoiled DNA molecules, Phys. Chem. Chem. Phys. 12 (2010) 14727–14734.
[12] S. Santos et al., Stability, resolution and ultra-low wear amplitude modulation atomic force microscopy of DNA: small amplitude small set-point imaging, Appl. Phys. Lett. 103 (2013) 063702.
[13] C. Rivetti, M. Guthold, C. Bustamante, Wrapping of DNA around the *E. coli* RNA polymerase open promoter complex, EMBO J. 18 (1999) 4464–4475.
[14] L. Mangiarotti et al., Sequence-dependent upstream DNA–RNA polymerase interactions in the open complex with λ_{PR} and λ_{PRM} promoters and implications for the mechanism of promoter interference, J. Mol. Biol. 385 (2009) 748–760.
[15] S. Kasas et al., *Escherichia coli* RNA polymerase activity observed using atomic force microscopy, Biochemistry 36 (1997) 461–468.
[16] M. Guthold et al., Direct observation of one-dimensional diffusion and transcription by *Escherichia coli* RNA polymerase, Biophys. J. 77 (1999) 2284–2294.
[17] C. Bustamante et al., Facilitated target location on DNA by individual *Escherichia coli* RNA polymerase molecules observed with the scanning force microscope operating in liquid, J. Biol. Chem. 274 (1999) 16665–16668.
[18] M. Endo et al., Direct visualization of the movement of a single T7 RNA polymerase and transcription on a DNA Nanostructure, Angew. Chem. 124 (2012) 8908–8912.
[19] N. Crampton et al., Collision events between RNA polymerases in convergent transcription studied by atomic force microscopy, Nucleic Acids Res. 34 (2006) 5416–5425.
[20] K.S. Murakami, S.A. Darst, Bacterial RNA polymerases: the wholo story, Curr. Opin. Struct. Biol. 13 (2003) 31–39.
[21] P. Cramer, Multi-subunit RNA polymerases, Curr. Opin. Struct. Biol. 12 (2002) 89–97.

[22] R.M. Saecker, M.T. Record Jr, P.L. Dehaseth, Mechanism of bacterial transcription initiation: RNA polymerase – promoter binding, isomerization to initiation-competent open complexes, and initiation of RNA synthesis, J. Mol. Biol. 412 (2011) 754–771.
[23] R.R. Burgess et al., Factor stimulating transcription by RNA polymerase, Nature 221 (1969) (1969) 43–46.
[24] N. Crampton et al., Imaging RNA polymerase–amelogenin gene complexes with single molecule resolution using atomic force microscopy, Eur. J. Oral Sci. 114 (2006) 133–138.
[25] R.A. Mooney, S.A. Darst, R. Landick, Sigma and RNA polymerase: an on-again, off-again relationship?, Mol Cell 20 (2005) 335–345.
[26] A.N. Kapanidis et al., Retention of transcription initiation factor σ70 in transcription elongation: single-molecule analysis, Mol. Cell 20 (2005) 347–356.
[27] G. Bar-Nahum, E. Nudler, Isolation and characterization of σ70-retaining transcription elongation complexes from *Escherichia coli*, Cell 106 (2001) 443–451.
[28] J.H. Roe, M.T. Record Jr, Regulation of the kinetics of the interaction of *Escherichia coli* RNA polymerase with the lambda PR promoter by salt concentration, Biochemistry 24 (1985) 4721–4726.
[29] Y. Wang, R.H. Austin, E.C. Cox, Single molecule measurements of repressor protein 1D diffusion on DNA, Phys. Rev. Lett. 97 (2006) 048302.
[30] J. Ellis et al., Direct atomic force microscopy observations of monovalent ion induced binding of DNA to mica, J. Microsc. 215 (2004) 297–301.
[31] S. Mantelli et al., Conformational analysis and estimation of the persistence length of DNA using atomic force microscopy in solution, Soft Matter 7 (2011) 3412–3416.
[32] S.E. Halford, An end to 40 years of mistakes in DNA-protein association kinetics?, Biochem Soc. Trans. 37 (2009) 343–348.
[33] G. Walter et al., Initiation of DNA-Dependent RNA synthesis and the effect of heparin on RNA polymerase, Eur. J. Biochem. 3 (1967) 194–201.
[34] Z. Shriver et al., Heparin and heparan sulfate: analyzing structure and microheterogeneity, Handb. Exp. Pharmacol. 207 (2012) 159–176.
[35] D.L. Rabenstein, Heparin and heparan sulfate: structure and function, Nat. Prod. Rep. 19 (2002) 312–331.
[36] B. Mulloy et al., NMR and molecular-modelling studies of the solution conformation of heparin, Biochem. J. 293 (1993) 849–858.
[37] S.R. Pfeffer, S. Stahl, M. Chamberlin, Binding of *Escherichia coli* RNA polymerase to T7 DNA. Displacement of holoenzyme from promoter complexes by heparin, J. Biol. Chem. 252 (1977) 5403–5407.
[38] G. Dieci, B. Fermi, M.C. Bosio, Investigating transcription re-initiation through *in vitro* approaches, Transcription 5 (2014) e27704.
[39] E.M. Prescott, N.J. Proudfoot, Transcriptional collision between convergent genes in budding yeast, Proc. Natl. Acad. Sci. U.S.A. 99 (2002) 8796–8801.
[40] B.P. Callen, K.E. Shearwin, J.B. Egan, Transcriptional interference between convergent promoters caused by elongation over the promoter, Mol. Cell 14 (2004) 647–656.
[41] K.E. Shearwin, B.P. Callen, J.B. Egan, Transcriptional interference – a crash course, Trends Genet. 21 (2005) 339–345.
[42] K. Sneppen et al., A mathematical model for transcriptional interference by RNA polymerase traffic in *Escherichia coli*, J. Mol. Biol. 346 (2005) 399–409.
[43] M.D. Abràmoff, P.J. Magalhães, S.J. Ram, Image processing with ImageJ, Biophotonics Int. 11 (2004) 36–42.
[44] C. Rivetti, M. Guthold, C. Bustamante, Scanning force microscopy of DNA deposited onto mica: equilibration versus kinetic trapping studied by statistical polymer chain analysis, J. Mol. Biol. 264 (1996) 919–932.
[45] P.E. Marszalek et al., The force-driven conformations of heparin studied with single molecule force spectroscopy, Biophys. J. 85 (2003) 2696–2704.
[46] G. Pavlov et al., Conformation of heparin studied with macromolecular hydrodynamic methods and X-ray scattering, Eur. Biophys. J. 32 (2003) 437–449.